

# Comparison of Pore Space Features by Thin Sections and X-Ray Microtomography

H. Alves, J. T. Assis, M. Gerales, I. Lima, and R. T. Lopes

**Abstract**—Microtomographic images and thin section (TS) images were analyzed and compared against some parameters of geological interest such as porosity and its distribution along the samples. The results show that microtomography ( $\mu$ CT) analysis, although limited by its resolution, have some interesting information about the distribution of porosity (homogeneous or not) and can also quantify the connected and non-connected pores, i.e., total porosity. TS have no limitations concerning resolution, but are limited by the experimental data available in regards to a few glass sheets for analysis and also can give only information about the connected pores, i.e., effective porosity. Those two methods have their own virtues and flaws but when paired together they are able to complement one another, making for a more reliable and complete analysis.

**Keywords**—Microtomography, petrographical microscopy, sediments, thin sections.

## I. INTRODUCTION

IN the field of geosciences, there is a large interest on analysis of the pore space and its characteristics, such as void space and pore dimension. Porosity is usually referred as the amount of void space on which fossil fuels, such as petroleum and gas, but also water, might be found. Some traditional techniques are often applied for evaluation and quantification, such as, thin sections or mercury intrusion porosimetry [1]-[3]. Although commonly used, those procedures are destructive which does not prevent future investigation, but comparison, in such objects because they have been already chemically or physically changed. Moreover, they also require intensive and tiresome work since those procedures are not automated and might be limited by the operator, especially in the case of point counting, which is a means of describing rocks and its void space in a quantitative way by thin sections.

Thin sections (TS) for microscopic materials investigation in transmitted and reflected light remains one of the most classic mineralogical methods of analysis in petrophysical researches. Thin sections provide an approach with identification of substances with relatively high spatial

resolution. It allows an estimate of chemical compositions and provides clues for understanding the history of the rock formation [4].

X-ray microtomography ( $\mu$ CT) is a technique already established for industrial use and its applications have been expanded to investigate pore network of potential reservoir rocks and sedimentary rocks [5]-[7]. Although  $\mu$ CT still has some issues concerning the spatial and density resolutions [8] which are not in pair with thin sections and mercury porosimetry techniques, and some issues concerning the appearance of artifacts and noise in the final image [9], it is a reliable laboratory examination that has been frequently used in the petroleum and gas field.  $\mu$ CT does not need intervention of the operator and the images evaluation can be performed automatically by several image processing algorithms of reconstruction and segmentation, which diminishes the work and influence of the operator, increasing comparison, reliability and reproducibility of the technique.

The aim of this work was to provide a comparison study between thin sections and  $\mu$ CT results of the void space of sediments by quantifying porosity, pore size and its distribution along the samples. The results show that  $\mu$ CT have several advantages over traditional methods and might become a standard method for geological analysis in the future. Even so,  $\mu$ CT shows best efficiency when paired with others techniques.

## II. METHODOLOGY

In this work three groups of sediment samples were used and they were named as 2MC1SC, 7AR155BA and VF4SE. Those acronyms refer to the location of origin, specifically Brazilian basins, where the samples were taken. In total 13 sub-samples (1cm<sup>3</sup> of volume for each sub-sample) were extracted from the original samples as follow: 4 samples from 2MC1SC group, 4 samples from 7AR155BA group and 5 samples from VF4SE group. All of them were scanned and then four thin sections of each original sample were made and analyzed.

$\mu$ CT of all samples were performed with a Skyscan/Bruker® [10] apparatus, model 1173, which is a high-energy system equipment to operate up to 130kV of energy and minimum resolution of 5 $\mu$ m. The detector is a flat panel type of 50 $\mu$ m pixel size. The acquisitions were carried out with a pixel size of 9.91 $\mu$ m, energy and current of 90kV and 88 $\mu$ A, respectively.

There are important settings in the acquisition procedure that can be performed by a combination of different parameters, such as, the rotation step, random movement

H. Alves, I. Lima, and R. T. Lopes are with the Nuclear Engineering Program, Federal University of Rio de Janeiro, Rio de Janeiro, Brazil (Phone: +55 21 25627311; e-mail: haimon.dlafis@gmail.com, inayacorrea@gmail.com, ricardo@lin.ufrj.br)

J. T. Assis is with the Mechanical Engineering Program, State University of Rio de Janeiro, Nova Friburgo, Brazil (Phone: +55 21 25332287; e-mail: joaquim@iprj.uerj.br).

M. Gerales is with the Geological Department, State University of Rio de Janeiro, Rio de Janeiro, Brazil (Phone: +55 21 25877601; e-mail: mauro.gerales@gmail.com).

compensation, frames number and beam hardening correction. In order to achieve better image quality, the samples were scanned over 360 degrees with a rotation step of 1 degree and the random movement parameter was set with amplitude (in number of detector lines) of 100, which can reduce ring artifacts in the reconstruction cross sections. A series of x-ray images at a frame rate of 5 frames per exposure time of 800 ms was performed, which allows to improve the image quality by averaging several images in every angular position. In order to reduce beam hardening effects, which appears because of a preferential absorption by the borders of the sample, a combination of two metallic filters was used: aluminum (1.0mm of thickness) and copper (0.15mm of thickness).

NRecon® (v.1.3.9.2) program and InstaRecon® engine (v.1.6.8.0) packages were used in order to reconstruct cross-section images [11], [12]. After reconstruction, image processing analysis was performed and the pore space was analyzed from all segmented data sets using CTAn® (v.1.13.2.0) [13] software. This software allows segmentation of different phases related to the attenuation coefficient and/or material density, image processing procedures and quantification of several morphometric 2D/3D parameters, such as porosity. In order to separate porosity from sediment matrix multi-level thresholding mode, for two different phases beyond the pore phase, was used, which is based on automatic Otsu's method [14], i.e., it is an automatic type of thresholding without manual interference. In this way, the binary selection (white voxels) determines which voxels are included in the volume of interest (VOI) that was set exactly equal to the boundary of the sample (ROI Shrink-Wrap). At this moment despeckle plug-in was also used in order to erase all false objects that do not favor the quantification procedure, being that all objects with less than 20 voxels were cut out; Finally, at the end of the image process, we have a stack of binary images in which white pixels represent the pore space and black pixels correspond to other sediment structures.

Thin sections were made in laboratory from the original samples from each group. They were cut in the middle of the sample with approximately 0.5cm using a diamond saw, placed in a glass sheet and polished with abrasive powder until its thickness achieved 30 $\mu$ m. After that the thin section was seen through a petrographical polarization microscope, Axioskop 40 with resolution up to 0.05 $\mu$ m using two polarized filters in order to monochromize the light (plain polarized natural light) [15]. The minerals optical properties of the sediments change perceived color and light intensity which passes through the glass sheet, allowing identification of mineral composition. Connected pores can be seen by means of a blue penetrating liquid. Porosity is usually evaluated by point counting polished thin sections under reflected light [16]. In this work, however, digital approach was used by digital scanning of the thin sections. For that purpose, a digital camera Canon G10 14.7 megapixels with a 28mm wide-angle lens coupled with an adaptor tube for Canon G10 Wide 52mm was used. Digital images with 4416 x 3312 pixels were obtained. After that, the same CTAn® software used in  $\mu$ CT

analysis was used here in order to perform the quantification of the penetrating liquid related to porosity. Since the histogram is not clearly defined on the blue penetrating liquid (some dark regions are misunderstood by the software) a manual thresholding was used. Although this method depends on the operator, it makes for a better segmentation on a basis of compensation. The same parameters were used as in  $\mu$ CT image analysis after the segmentation procedure. The analysis of each thin section, however, was evaluated by 2D analysis, since there was no stack of images but only one digital image for each thin section.

Fig. 1 shows an example of the comparison between one digital scanning thin section and one  $\mu$ CT cross-section from the 7AR155BA group.

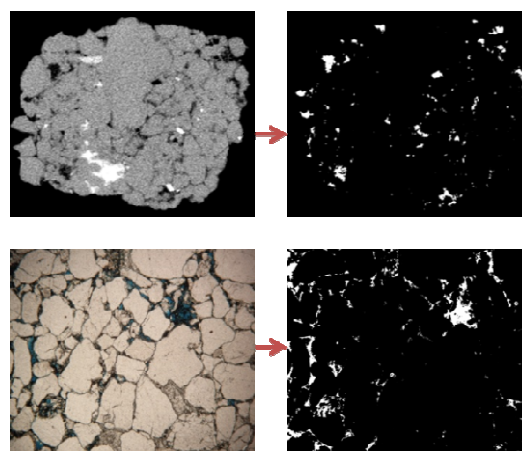


Fig. 1 Images of CT and thin sections, respectively, against its segmented image

### III. RESULTS

Tables I and II show  $\mu$ CT and thin section porosity results, respectively. In Table I, it can be seen that all calculated values by  $\mu$ CT are almost the same for 2D and 3D quantification. 2D quantification is calculated using data of each 2D-slice of  $\mu$ CT images, as 3D quantification does the entire procedure using the whole volume of data, i.e., the full stack of  $\mu$ CT images. Mean value 2D is the mean calculated value of porosity by using all values of porosity obtained for each 2D-slice. It can give an idea of how much variation the 2D data shows when compared to 2D and 3D quantification. As it will be shown, the distribution of porosity (Fig. 2) is not homogeneous, or almost, for all samples. Even so the higher values makes up for the lower values, resulting in a similar value of mean value 2D for 2D and 3D quantification.

In Table II, it can be seen that all calculated values for TS. Although the results do not show homogeneous distribution, it is necessary to point it out that thin sections are not as representative as  $\mu$ CT since it is difficult to compare few thin sections and the whole volume of interest of the sample, which amounts for thousands of slices. One could imagine the evaluation of thousands of thin sections when comparing to  $\mu$ CT.

Fig. 2 shows distribution of  $\mu$ CT porosity through the Z-axis of each sample of each group. Some samples have an almost uniform distribution of porosity, with values calculated by  $\mu$ CT not very far from the mean value, throughout them which makes for mean values that are very close to the ones calculated from 2D and 3D.

TABLE I  
 POROSITY VALUES BY  $\mu$ CT

$\mu$ CT	Porosity Values (%)		
7AR155BA Samples	2D	3D	2D Mean Value
1	3.332	3.255	3.302
2	4.006	3.927	4.010
3	4.413	4.319	4.416
4	3.961	3.874	3.961
2MC1SC Samples	2D	3D	2D Mean Value
1	1.465	1.344	1.335
2	1.439	1.339	1.433
3	1.418	1.303	1.451
4	1.395	1.287	1.425
VF4SE Samples	2D	3D	2D Mean Value
1	0.0066	0.0056	0.0065
2	0.0057	0.0048	0.0058
3	0.1720	0.1586	0.1744
4	0.0142	0.0127	0.0157
5	0.0316	0.0275	0.0367

TABLE II  
 POROSITY VALUES BY DIGITAL SCANNING THIN SECTIONS

$\mu$ CT	Porosity Values (%)	
7AR155BA Thin Sections	2D	3D
1	7.014	6.748
2	5.561	5.316
3	4.642	4.442
4	6.429	6.224
2MC1SC Thin Sections	2D	3D
1	11.59	11.23
2	15.17	14.73
3	22.39	21.96
4	19.25	18.82
VF4SE Thin Sections	2D	3D
1	0.00002	0.00001
2	0.00935	0.00738
3	0.00478	0.00340
4	0.02865	0.02212

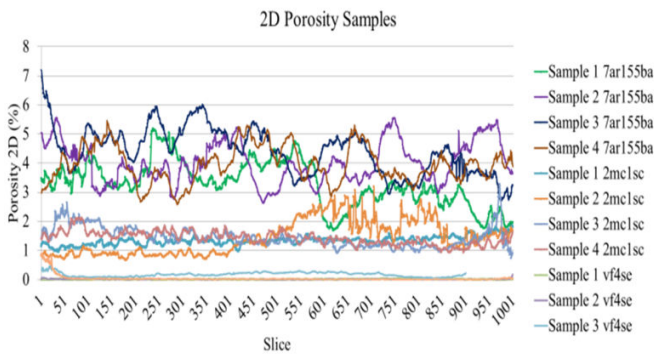


Fig. 2 Distribution of porosity throughout all samples

Figs. 3-5 show 3D images of pores and its size.

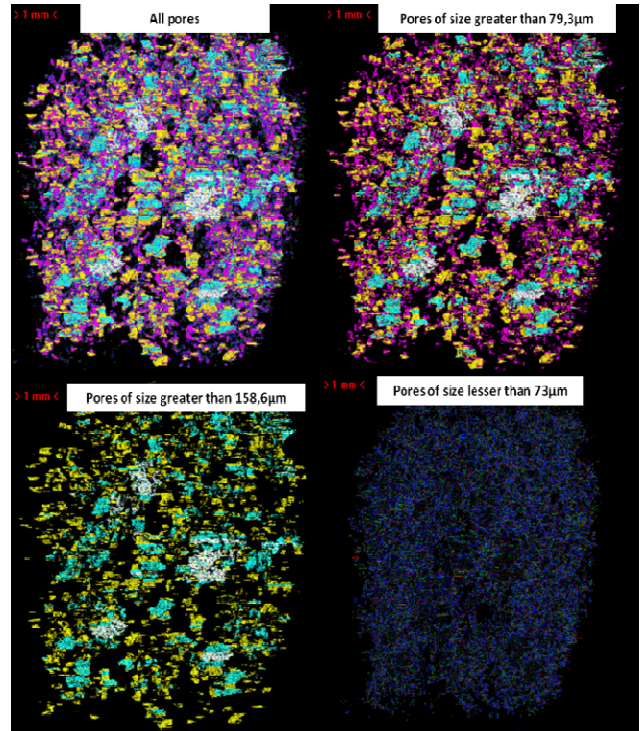


Fig. 3 3D visualizations of sample 1 of 7ar155ba group

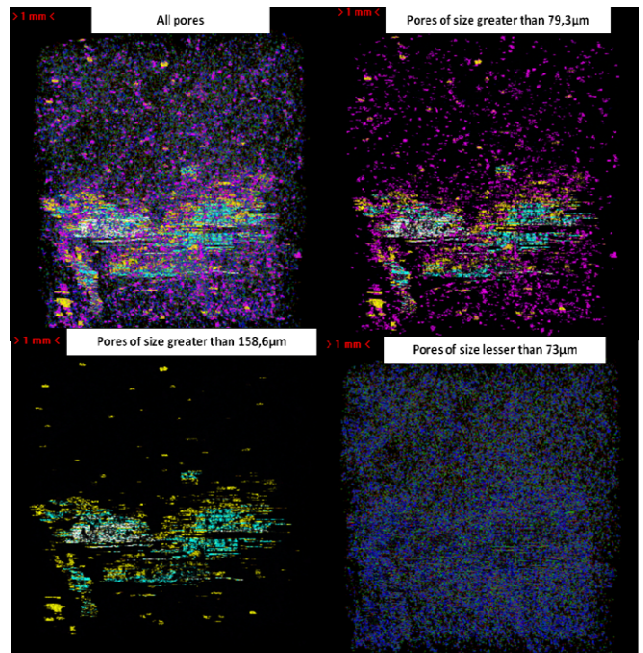


Fig. 4 3D visualization of sample 2 of 2mc1sc group



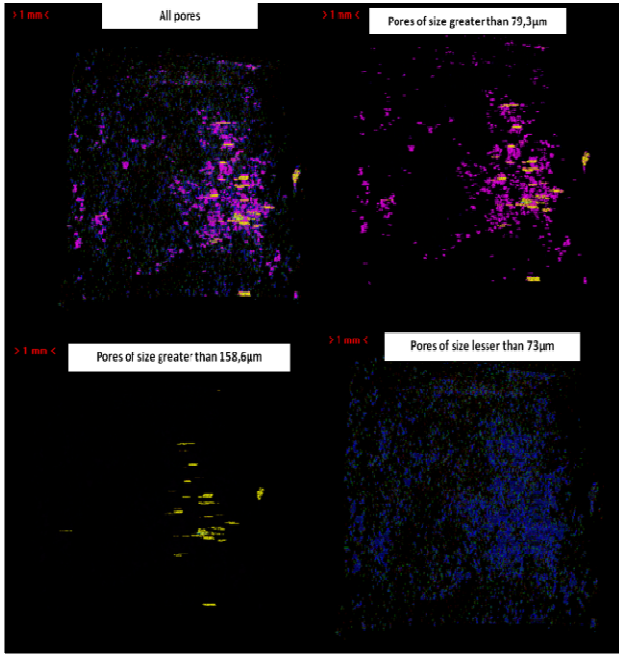


Fig. 5 3D visualization of sample 3 of vf4se group

It is possible to see that pores of greater size can be easily distinguished since they are not as large in numbers as smaller pores, which are not possible to distinguish but show signs of homogeneous distribution throughout the samples. In some particular samples there are small regions with accumulated pores which might explain odd peaks on the distribution of porosity.

Figs. 6-8 show 2D images of TS and its segmented images.

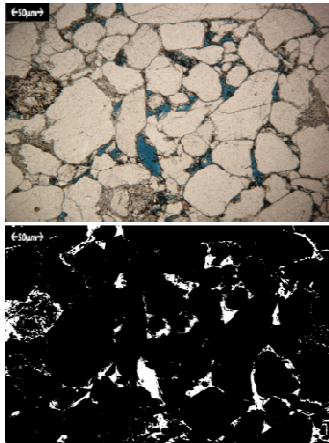


Fig. 6 Segmented TS of 7ar155ba group

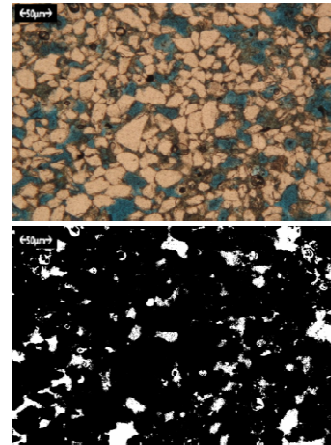


Fig. 7 Segmented TS of 2mc1sc group

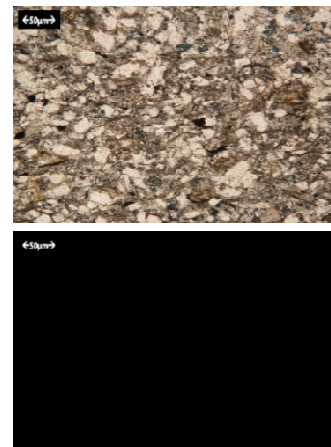


Fig. 8 Segmented TS of vf4se group

Not all regions saturated by the blue penetrating liquid can be segmented by the software since the divisions of RGB composition are not as clear as they seem to be on the images. That explains why some darker spots are also segmented, although not as frequent as the liquid. It is necessary to go for a balance between optimum thresholding of RGB color palette and minimum presence of “noise”, i.e., darker spots, as to avoid miscalculations, e.g., overestimation or underestimation. Figs. 9-11 show comparison between  $\mu$ CT and TS of obtained values of porosity.

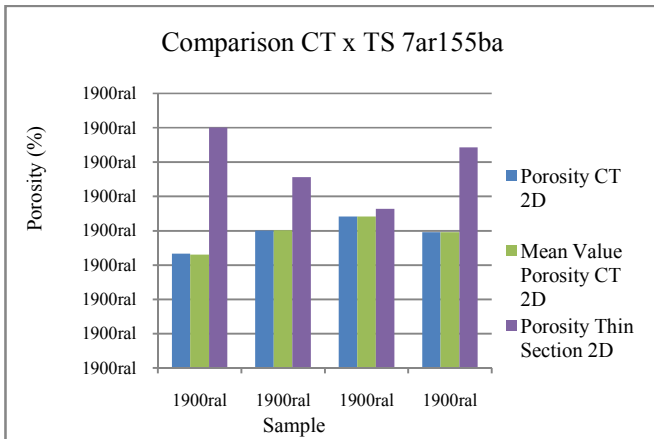


Fig. 9 Comparison between  $\mu$ CT and TS results of 7ar155ba group

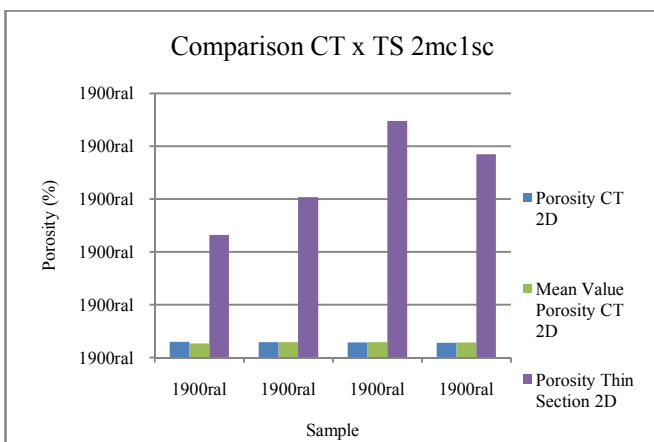


Fig. 10 Comparison between  $\mu$ CT and TS results of 2mc1sc group

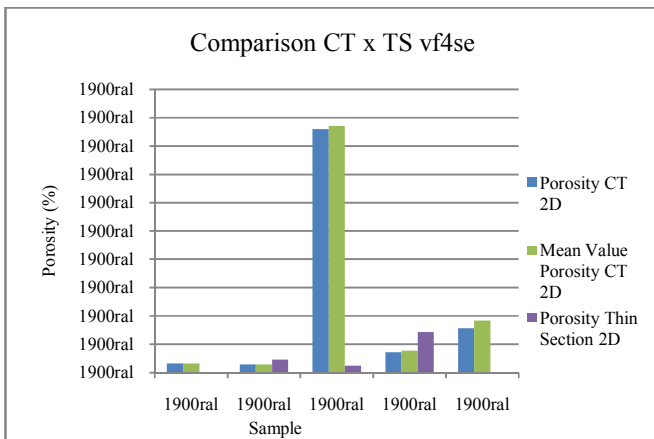


Fig. 11 Comparison between  $\mu$ CT and TS results of vf4se group

Samples of groups 7ar155ba and 2mc1sc show all porosity values of thin sections bigger than porosity values obtained through  $\mu$ CT. This should be expected since thin sections have a better resolution than  $\mu$ CT and the penetrating liquid can reach pores of smaller sizes too. In the case of group 2mc1sc there is a higher discrepancy because of the connectivity, existent on the pore matrix. If pores are more connected, then the penetrating liquid have means of reaching far more pores,

though increasing the values of porosity. If there are no connections, then thin sections will provide almost no porosity which happens in samples from group vf4se. Most of the samples have fewer connections and that is why porosity values obtained through  $\mu$ CT are greater.

Samples of group 7ar155ba were found to be, at its essence, homogeneous.  $\mu$ CT showed values of porosity a little smaller than those obtained by TS. That shows little difference in porosity even on a smaller scale that of micrometers. The main difference is probably because of the resolution of the  $\mu$ CT. Even with few TS evaluated, the results are very similar which reaffirms the hypothesis that the samples are homogeneous.

Samples of group 2mc1sc show large variations of porosity between  $\mu$ CT and TS but also amongst TS. This fact probably indicates two major things: the first one is that those samples have many pores with smaller sizes than micrometers which cannot be identified by  $\mu$ CT; the second one is that those samples are not heterogeneous on a scale beyond the actual capacity of  $\mu$ CT, i.e., are not heterogeneous at all. Also, one can conclude that those samples have higher connectivity than the other groups.

Samples of group vf4se show little variation and all samples have almost no porosity for both techniques. The sample 3 shows greater porosity than the others on  $\mu$ CT results. That indicates that samples have almost no connectivity and this one probably have just a few non-connected pores. Even so the porosity of samples of group vf4se is not greater than 0.18% which is a really low value and can be thought of non-existent for practical purposes.

#### IV. CONCLUSION

The results obtained through  $\mu$ CT have its limitations related, primarily, to the resolution. Although much better than earlier years, it is still not enough to reach pores of dimension of nanometers.  $\mu$ CT is able to identify pores connected and non-connected, a feature TS does not possess. It can also give values related to each slice which can be compared to thousands TS and values related to a 3D perspective. Since it is not able to give information on anything smaller than a few micrometers, its comparison can only be done with that information in mind. Quantification of porosity by  $\mu$ CT gives distribution of porosity on all extent of the sample which tells us if there is a homogeneous or heterogeneous distribution and how that distribution happens. It is also expected that values of porosity given by  $\mu$ CT are smaller than those by TS, which is not always the case. Sometimes a sample can be very porous but since TS needs connectivity, it might not show the reality when quantifying the segmented images. We also need to remember that TS usually uses just a few glass sheets for evaluation and they might not be representative of the distribution of porosity. That being said, it would take several TS of the sample to make for a better comparison which would be very laborious, tiresome and it would take a really long time.  $\mu$ CT allows for much more information on a sample in a few hours showing that  $\mu$ CT is a better technique in many ways and it is still improving.

#### ACKNOWLEDGMENT

The authors of this work would like to thank CNPq for the financial support.

#### REFERENCES

- [1] Thomas R. Elliot, Richard J. Heck, "Comparison of optical and X-ray CT technique for void analysis in soil thin section", *Geoderma*, vol. 141 (1-2), 2007, pp. 60-70.
- [2] P.J. Armitage , R.H. Worden, D.R. Faulkner, A.C. Aplin, A.R. Butcher, J. Iliffe, "Diagenetic and sedimentary controls on porosity in Lower Carboniferous fine grained lithologies, Krechba field, Algeria: A petrological study of a caprock to a carbon capture site", *Marine and Petroleum Geology*, vol.27 (7), 2010, pp. 1395-1410.
- [3] Desbois, G., Urai, J.L., Kukla, P.A., Konstanty, J., Baerle, C., "High-resolution 3D fabric and porosity model in a tight gas sandstone reservoir: A new approach to investigate microstructures from mm- to nm-scale combining argon beam cross-sectioning and SEM imaging", *Journal of Petroleum Science and Engineering*, vol. 78 (2), 2011, pp. 243-257.
- [4] Terry Moxon, "Studies on Agate", 2009, Terra Publications.
- [5] M. Van Geet, R. Swennen, M. Wevers, "Quantitative analysis of reservoir rocks by microfocuss X-ray computerised tomography", *Sedimentary Geology*, vol. 132, 2000, pp. 25–36.
- [6] M. Van Geet, D. Lagrou , R. Swennen , "Porosity measurements of sedimentary rocks by means of microfocuss X-ray computed tomography", *Sedimentary Geology*, vol. 132 (1-2), 2003, pp. 25-36.
- [7] M. F. S. Oliveira, I. Lima, L. Borghi, R. T. Lopes, "X-ray microtomography application in pore space reservoir rock", *Applied Radiation and Isotopes*, vol. 70 (7), 2012, pp. 1376–1378.
- [8] A.C. Machado, I. Lima, R.T. Lopes, "Effect of 3d computed microtomography resolution on reservoir rocks", *Radiation Physics and Chemistry*, 2013, <http://dx.doi.org/10.1016/j.radphyschem.2012.12.029>.
- [9] K. Remeysen, R. Swennen, "Application of microfocuss computed tomography in carbonate reservoir characterization: Possibilities and limitations", *Marine and Petroleum Geology*, vol. 25, 2008, pp. 486–499.
- [10] Skyscan 1173, 2013. "User Guide", SkyScan/Bruker Micro-CT, Kartuizerweg 3B 2550 Kontich, Belgium.
- [11] NRecon, 2013. SkyScan/Bruker Micro-CT, Kartuizerweg 3B 2550 Kontich, Belgium.
- [12] InstaRecon®, 2013. CBR Premium 12-8K™, InstaRecon, Champaign, IL, USA.
- [13] CTAnalyser, 2013, "The User's Guide", Skyscan/Bruker micro-CT, Kartuizerweg 3B 2550 Kontich, Belgium.
- [14] Nobuyuki Otsu, "A threshold selection method from gray-level histograms", *IEEE Transactions on Systems, Man and Cybernetics*, vol. smc-9, no.1,1979, pp.62-66.
- [15] MicroscopyU, "Introduction to Polarized Light Microscopy", <http://www.microscopyu.com/articles/polarized/polarizedintro.html>, last viewed: March 2013.
- [16] JavadGhiasi-Freez, ImanSoleimanpour, Ali Kadkhodaie-Ilkhchi, Mansur Ziaii, Mahdi Sedighi, Amir Hatampour, "Semi-automated porosity identification from thin section images using image analysis and intelligent discriminant classifiers" 2012, *Computer & Geosciences*, vol. 45, pp. 36-45.